SRRS Effects on ICF Laser Drive Beam with the Variation of Pump Light Distribution on Space

Ying Liu[1, 2], Dianyang Lin[2], Zhiwei Lu[2], Weiliang Zeng[1,*]

[1]*School of Mathematics Science, Harbin Normal University, Harbin 150025, China*
[2]*National Key Laboratory of Tunable Laser Technology, Harbin Institute of Technology, Harbin 150001, China*
* zengcongluo@126.com

Abstract

Tens to hundreds of output high power lasers from ICF (inertial confinement fusion) device, generally need to propagate through a long air path before they reach the target chamber. During the process, interaction between the high power pulse laser and air molecules emerges. Once the SRRS (stimulated rotational Raman scattering) threshold was reached, the SRRS effect would result in the loss of laser energy, the decrease of laser beam quality, or unable to reach the target. Further the transmitted laser would enter the multipliers as fundamental beam, then the conversion efficiency of triple-harmonic would be affected, even cause the destroy of frequency multiplication crystal. In order to improve the output ability, beam quality and control ability of the ICF high power laser drive, ultimately achieve the fusion ignition success, the SRRS effect must be suppressed. Based on SRRS four-dimensional mathematical model which conforms to current ICF experiment conditions, the longitudinal and horizontal rules of SRRS effect on ICF laser drive beam with the variation of pump light distribution on space was obtained. The research provided a support for the parameters choice of ICF laser drive and the optimization of output beam quality.

Keywords: ICF laser drive beam; stimulated rotational Raman scattering; four-dimensional mathematical

1. Introduction

It is necessary for tens to hundreds of output high power lasers from ICF (inertial confinement fusion) device, generally need to propagate through a long air path before they reach the target chamber. During the process, interaction between the high power pulse laser and air molecules emerges. Once the SRRS (stimulated rotational Raman scattering) threshold was reached, the SRRS effect would result in the loss of laser energy, the decrease of laser beam quality, or unable to reach the target. Further the transmitted laser would enter the multipliers as fundamental beam, the conversion efficiency of triple-harmonic would be affected, even cause the destroy of frequency multiplication crystal. In order to improve the output ability, beam quality and control ability of the ICF high power laser drive, ultimately achieve the fusion ignition success, the SRRS effect must be suppressed.[1]

For the conventional SRRS suppression methods, as replaced air by vacuum or inert gas, might increase the project cost and maintenance fee, as well as the follow-up maintenance difficulties. In addition, vacuum-ultraviolet effect and pollution effect might happen in the progress, results in adverse effects on quartz crystal and optical components. Comparing with traditional ICF drives, the new generation of ICF drives

---

Weiliang Zeng is the corresponding author.

provide higher power and more beams, it's more important to solve the SRRS problem. In summary, to carry out the quantitative research of SRRS effect on ICF laser drive beam in air or other medium is very necessary.

This paper focused on the physical characteristics of SRRS effect on ICF laser drive combining with current experimental situation in the condition of different spatial distribution of ICF pump light.

2. Theoretical Analysis—SRRS Mathematics Model

Maxwell-Bloch-Langevin equations was used to describe the SRRS process of high power laser propagating through long distance in air by Rochester University of USA, that spontaneous Raman scattering generated first, then it could be regarded as seed light to be stimulated amplified in the next propagation.

Maxwell-Bloch-Langevin equations describe the whole coupling process of SRRS. Rochester University of U.S.A. used it to describe SRRS in 1993. The model included nonlinear polarization of medium, attenuation of pump light, production and amplification of Stokes light and which had been checked over in experiments on OMEGA device. We would use the same equations in this paper.

$$[\nabla_\perp^2 + 2ik_L \frac{\partial}{\partial z}]E_L = -2\kappa_3 k_L Q E_S \tag{1}$$

$$[\nabla_\perp^2 + 2ik_S \frac{\partial}{\partial z}]E_S = 2\kappa_2 k_S Q^* E_L \tag{2}$$

$$\frac{\partial Q^*}{\partial t} = -\Gamma Q^* + i\kappa_1 E_L^* E_S + F^* \tag{3}$$

Eq. (1) is the equation of pump light attenuation;

Eq. (2) is the equation of Stokes light production and amplification;

Eq. (3) is the equation about nonlinear polarization of medium;

where, E_L is the complex amplitude of pump light; E_S is the complex amplitude of Stokes light; Q is dielectric polarization; k_L is the wave number of pump light; k_S is the wave number of Stokes light; $\kappa_1, \kappa_2, \kappa_3$ are dielectric gain constants (coupling coefficients).

$$\begin{aligned} \kappa_1 &= \sqrt{\frac{\Gamma c g}{8\pi^2 n\hbar\omega_s}} \\ \kappa_2 &= \kappa_3 = \left(\frac{2\pi n\hbar\omega_s}{c}\right)\cdot\kappa_1^* \end{aligned} \tag{4}$$

Where, Γ is Raman bandwidth; F is the random force caused by collision in the direction of pump propagation; g is the steady-state gain coefficient; ω_s is the frequency of Stokes light; n is the number of Raman activated atoms; $\hbar$ is Planck constant; * is Complex conjugation.

Eq. (1) and Eq. (2) defines the diffraction and medium polarization influence on light field E_L, E_S respectively.

Eq. (1) and Eq. (2) indicate that they are in the same coordinate system of light speed.

Eq. (3) defines the instantaneous state of medium polarization by product of light field and random collision force F. It represents the linear relationship between Q and two driving forces.

3. The Four-Dimension Simulation Results

Base on previous research on SRRS of other scientists, combining with the current ICF experiment conditions, the four-dimensional simulation research of SRRS effects produced by ICF high power laser beam propagating in air through long-distance were carried out, we focused on the effect rules of SRRS on output beam quality with the variation of pump light spatial distribution.

Table 1. Calculation Parameters

Wavelength of the incident pump light	351.1 *nm*
Wavelength of Stokes light	352.04 *nm*
Intensity of initial pump light	2 *GW/cm²*
Raman line width	7.52×10^9 *Hz*
Raman gain coefficient	6.76×10^{-12} *cm/W*
Beam aperture	28 *cm*
Transmission distance	18 *m*
Raman activate atoms	2.234×10^{19} *cm⁻³*
Pulse width of pump light	3 *ns*

When the time domain distribution of pump light is 18-order super-Gaussian, the spatial distribution of pump light changes from 10 to 30 order super-Gaussian, the calculation and simulation results are as following.

3.1. When the Spatial Distribution of Pump Light is 10-Order Super-Gaussian

Figure 1 showed the three-dimensional intensity distribution of Q, pump light and Stokes light when spatial distribution of pump light was 10-order super-Gaussian, it could reflect the whole SRRS process clearly.

During the SRRS effect, the spontaneous Stokes light would always have a delay at time comparing with pump light. Then spontaneous Stokes light continued to be amplified as seed light, the whole SRRS process was the attenuation of pump light and the growth of Stokes light, they had a relationship of mutual growth and decline. When the propagation distance was 18m, the maximum Stokes light intensity had reached 2.067 GW/cm^2 at the end.
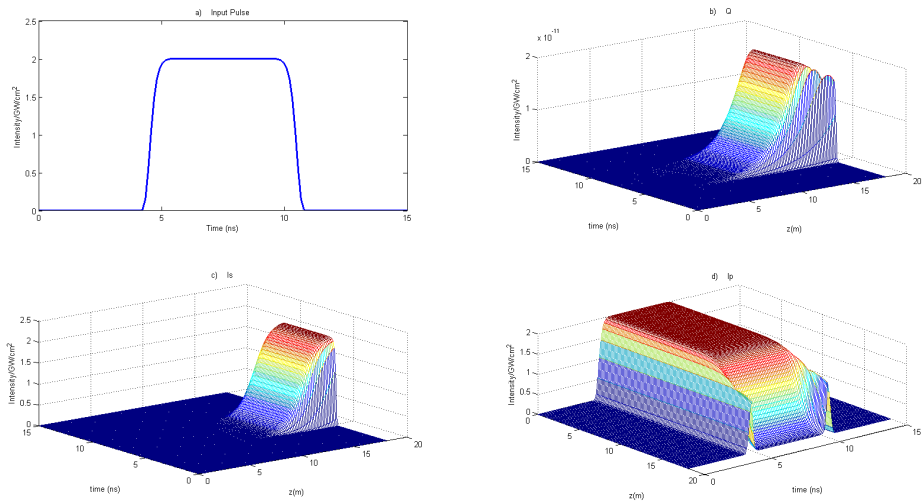
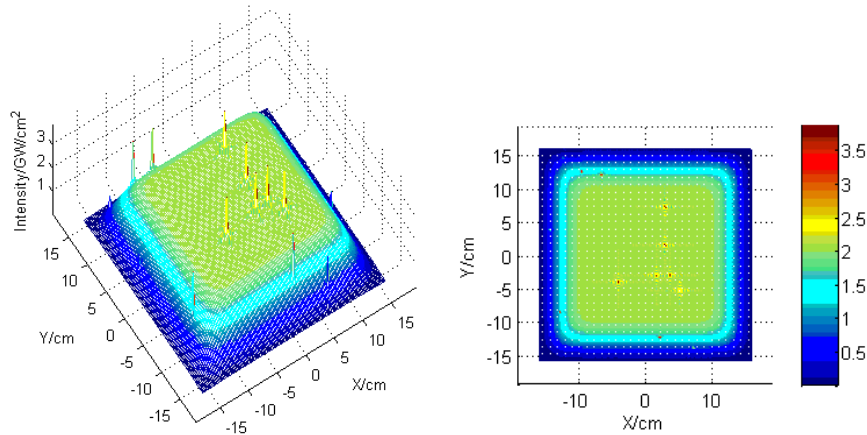a) The time domain intensity distribution
of initial pump light

b) The time-space domain intensity
distribution of Q throughout the process

c) The time-space domain intensity
distribution of Stokes light

d) The time-space domain intensity
distribution of pump light
throughout the process
throughout the process

Figure 1. The Calculated Intensity Distribution of *Q*, Pump Light and Stokes Light when the Spatial Distribution of Pump Light was 10-Order Super-Gaussian

Figure 2 was the three-dimension output light intensity distribution after SRRS when the pump light spatial distribution was 10 order super-Gaussian, the average light intensity was about 2.101 *GW/cm²*, large modulation of light intensity appeared suddenly, it was caused by the noise in initial pump light propagating process which was amplified throughout the SRRS process. It could be seen that diffraction effect appeared on output light edge, and the diffraction pattern distributed symmetrically.
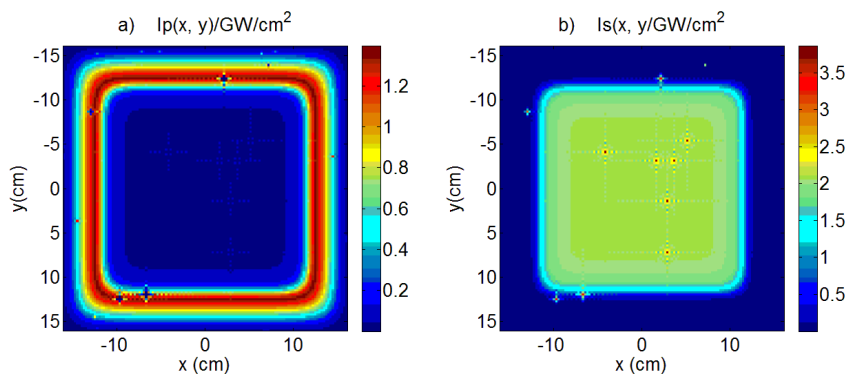
a) The three-dimension intensity distribution of output laser after SRRS

b) The transverse intensity distribution of output laser after SRRS

Figure 2. The Intensity Distribution of Output Laser after SRRS when the Spatial Distribution of Pump Light was 10-Order Super-Gaussian

Figure 3 was the transverse intensity distribution of output pump and Stokes light after SRRS when the pump light spatial distribution was 10 order super-Gaussian, it could be seen that the light intensity modulation occurred on output Stokes light cross-sections, that the noise generated as the initial pump light injection, then it was amplified through the SRRS process. It could be seen that where was the attenuation of pump light where was the growth of Stokes light, they had a relationship of mutual growth and decline. Diffraction occurred around the pump and Stokes beam again, comparing with Stokes beam, the diffraction of pump light was more obvious. The average laser intensity of the middle part of the output pump light beam was 0.03122 GW/cm^2; the width of its edge diffraction zone was about 2.01 cm.

a) The transverse intensity distribution of output pump light

b) The transverse intensity distribution of output Stokes light

Figure 3. The Transverse Intensity Distribution of Output Pump and Stokes Light after SRRS when the Spatial Distribution of Pump Light was 10-Order Super-Gaussian

As Figure 4 showed the relationship between gIL and SRRS conversion rate when the spatial distribution of pump light was 10 order super-Gaussian. When gIL was about

16.92, the corresponding SRRS conversion rate was 1%, that is the SRRS threshold. When propagation distance was 18 m, SRRS conversion rate was 36.87% at the end.
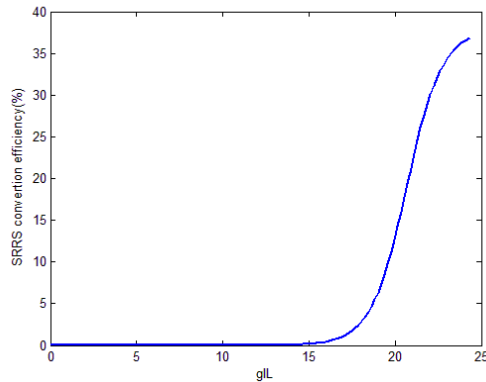

Figure 4. The Relationship Graph of SRRS Conversion Rate and gIL when the Spatial Distribution of Pump Light was 10-Order Super-Gaussian

3.2. When Spatial Distribution of the Pump Light was 22 Order Super-Gaussian

Figure 5 showed the three-dimensional intensity distribution of Q, pump light and Stokes light when spatial distribution of pump light is 22-order super-Gaussian, it could reflect the whole SRRS process clearly.

During the SRRS effect, the spontaneous Stokes light would always have a delay at time comparing with pump light. Then spontaneous Stokes light continued to be amplified as seed, the whole SRRS process was the attenuation of pump light and the growth of Stokes light, they had a relationship of mutual growth and decline. When the propagation distance was 18m, the maximum Stokes light intensity had reached 2.056 GW/cm^2 at the end.
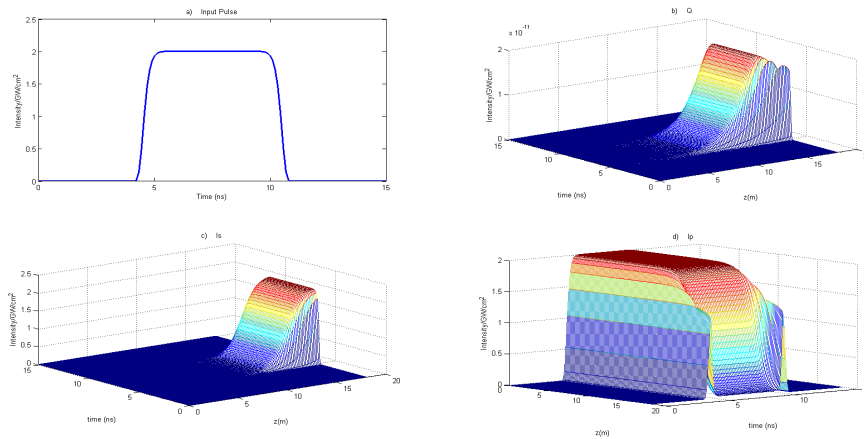
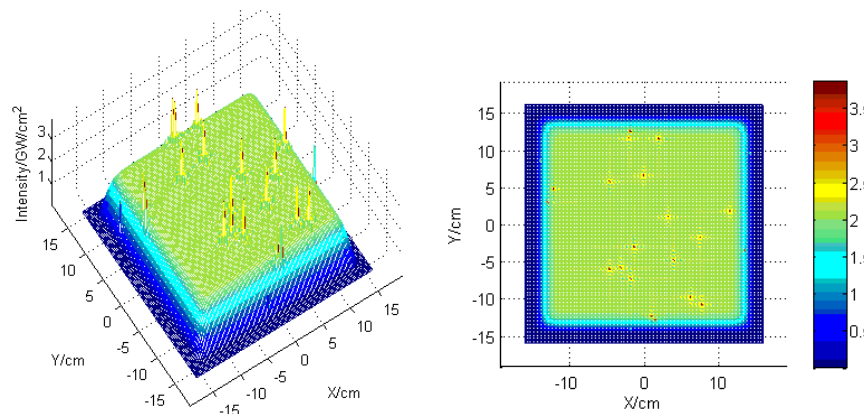a) The time domain intensity distribution of initial pump light

b) The time-space domain intensity distribution of Q throughout the process

c) The time-space domain intensity distribution of Stokes light throughout the process

d) The time-space domain intensity distribution of pump light throughout the process

Figure 5. The Calculated Intensity Distribution of *Q*, Pump Light and Stokes light when the Spatial Distribution of Pump Light was 22-order Super-Gaussian

Figure 6 was the three-dimension output light intensity distribution after SRRS when the pump light spatial distribution was 22 order super-Gaussian, the average light intensity was about 2.097 *GW/cm²*, large modulation of light intensity appeared suddenly, it was caused by the noise in initial pump light propagating process which was amplified throughout the SRRS process. It could be seen that diffraction effect appeared on output light edge, and the diffraction pattern distributed symmetrically.
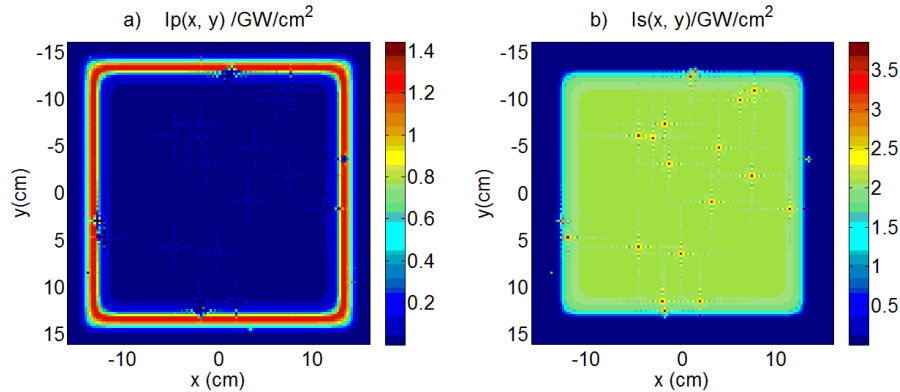

a) The three-dimension intensity distribution of output laser after SRRS

b) The transverse intensity distribution of output laser after SRRS

Figure 6. The Intensity Distribution of Output Laser after SRRS when the Spatial Distribution of Pump Light was 22-Order Super-Gaussian

Figure 7 was the transverse intensity distribution of output pump and Stokes light after SRRS when the pump light spatial distribution was 22 order super-Gaussian, it could be

seen that the light intensity modulation occurred on output Stokes light cross-section, that the noise generated as the initial pump light injection, then it was amplified through the SRRS process. It could be seen that where was the attenuation of pump light where was the growth of Stokes light, they had a relationship of mutual growth and decline. Diffraction occurred around the pump and Stokes beam again, compared with Stokes beam, the diffraction of pump light was more obvious. The average laser intensity of the middle part of the output pump light beam was 0.03204 *GW/cm^2*; the width of its edge diffraction zone was about 1.26 cm.

a) The transverse intensity distribution of output pump light

b) The transverse intensity distribution of output Stokes light

Figure 7. The Transverse Intensity Distribution of Output Pump and Stokes Light after SRRS when the Spatial Distribution of Pump Light was 22-Order Super-Gaussian

As Figure 8 showed the relationship between gIL and SRRS conversion rate when the spatial distribution of pump light was 22 order super-Gaussian. When gIL was about 16.92, the corresponding SRRS conversion rate was 1%, that is the SRRS threshold. When propagation distance was 18 m, SRRS conversion rate was about 36.87% at the end.
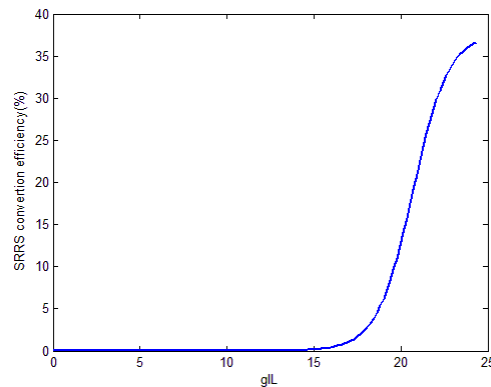

Figure 8. The Relationship Graph of SRRS Conversion Rate and gIL when the Spatial Distribution of Pump Light was 22-Order Super-Gaussian

3.3. When the Spatial Distribution of Pump Light is 30-Order Super-Gaussian

Figure 9 showed the three-dimensional intensity distribution of Q, pump light and Stokes light when spatial distribution of pump light was 30-order super-Gaussian, it could reflect the whole SRRS process clearly.

During the SRRS effect, the spontaneous Stokes light would always have a delay at time comparing with pump light. Then spontaneous Stokes light continued to be amplified as seed, the whole SRRS process was the attenuation of pump light and the growth of Stokes light, they had a relationship of mutual growth and decline. When the propagation distance was 18m, the maximum Stokes light intensity had reached 2.005 *GW/cm²* at the end.
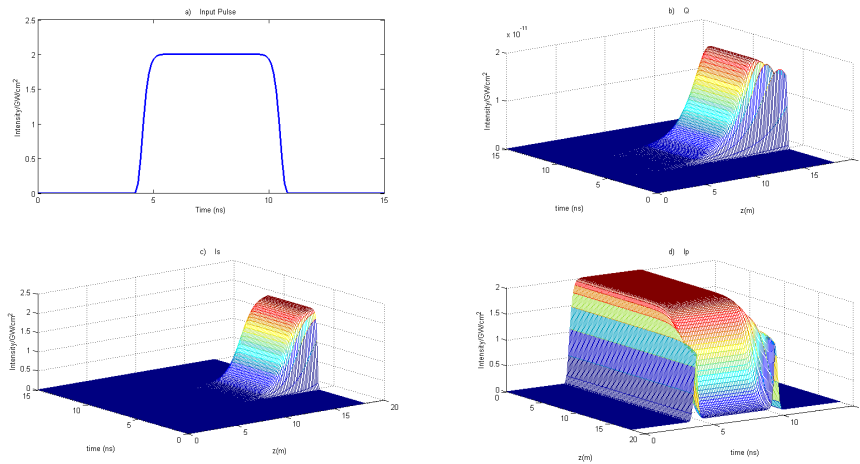
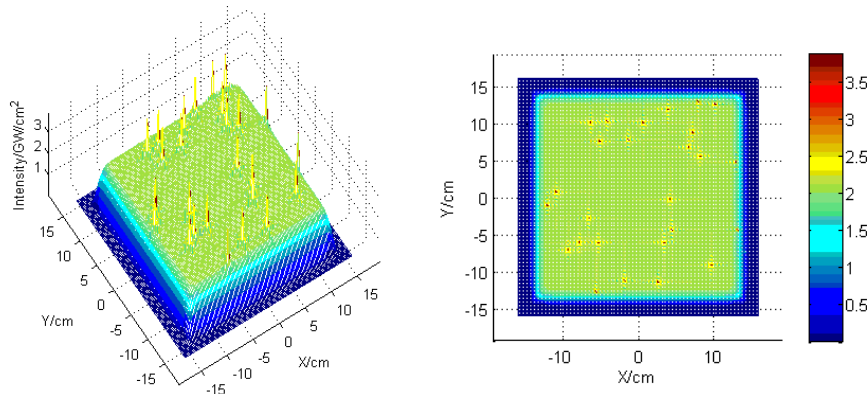a) The time domain intensity distribution of initial pump light

b) The time-space domain intensity distribution of Q throughout the process

d) The time-space domain intensity distribution of pump light throughout the process

c) The time-space domain intensity distribution of Stokes light throughout the process

Figure 9. The Calculated Intensity Distribution of Q, Pump Light and Stokes Light when the Spatial Distribution of Pump Light was 30-Order Super-Gaussian
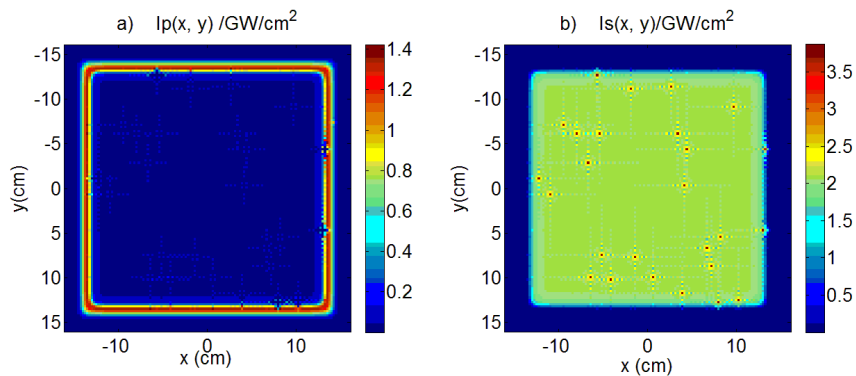
Figure 10 was the three-dimension output light intensity distribution after SRRS when the pump light spatial distribution was 30 order super-Gaussian, the average light intensity was about 2.087 *GW/cm²*, large modulation of light intensity appeared suddenly, it was caused by the noise in initial pump light propagating process which was amplified throughout the SRRS process. It could be seen that diffraction effect appeared on output light edge, and the diffraction pattern distributed symmetrically.

a) The three-dimension intensity distribution of output laser after SRRS

b) The transverse intensity distribution of output laser after SRRS

Figure 10. The Intensity Distribution of Output Laser after SRRS when the Spatial Distribution of Pump Light was 30-order Super-Gaussian

Figure 11 was the transverse intensity distribution of output pump and Stokes light after SRRS when the pump light spatial distribution was 30 order super-Gaussian, it could be seen that the light intensity modulation occurred on output Stokes light cross-section, that the noise generated as the initial pump light injection, then it was amplified through the SRRS process. It could be seen that where was the attenuation of pump light where was the growth of Stokes light, they had a relationship of mutual growth and decline. Diffraction occurred around the pump and Stokes beam again, compared with Stokes beam, the diffraction of pump light was more obvious. The average laser intensity of the middle part of the output pump light beam was 0.03204 GW/cm^2; the width of its edge diffraction zone was about 1 cm.

a) The transverse intensity distribution of output pump light

b) b) The transverse intensity distribution of output Stokes light

Figure 11. The Transverse Intensity Distribution of Output Pump and Stokes Light after SRRS when the Spatial Distribution of Pump Light was 30-Order Super-Gaussian

As Figure 12 showed the relationship between gIL and SRRS conversion rate when the spatial distribution of pump light was 30 order super-Gaussian. When gIL was about 16.92, the corresponding SRRS conversion rate was 1%, that is the SRRS threshold.

When propagation distance was 18 m, SRRS conversion rate was about 36.87% at the end.
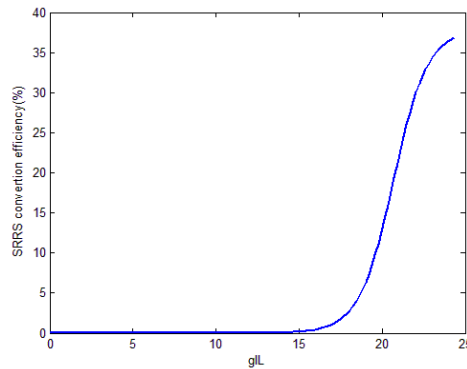

Figure 12. The Relationship Graph of SRRS Conversion Rate and gIL when the Spatial Distribution of Pump Light was 30-Order Super-Gaussian

4. Conclusion

After SRRS four-dimension simulation, rules of SRRS effects on ICF beam quality with the variation of pump light space distribution were got: The space distribution of the pump light varied from 10-order super-Gaussian to 30-order super-Gaussian, neither the SRRS threshold nor the SRRS conversion rate at propagation end would change. The transverse intensity distribution graph of output light showed that: as the order of super-Gaussian increased, the width of output pump light diffraction edge zones decreased.

Acknowledgements

References

[1]   Ying Liu, Dianyang Lin, Zhiwei Lu. Digest Journal of Nanomaterials and Biostructures. 2, 7 **(2012)**
[2]   Ying Liu, Dianyang Lin, Zhiwei Lu. "Numerical Simulation of Different Aperture ICF High Power Ultraviolet Laser Propagating through a Long Air Path," OPTIK. 17, 124 **(2013)**
[3]   Ying Liu, Dianyang Lin, Zhiwei Lu. Journal of Optoelectronics and Advanced Materials. 1–2, 16 **(2014)**
[4]   M.A.Henesian, C.D.Swift and J.R.Murray. Opt. Lett. 11, 10 **(1985)**
[5]   [M.A.Henesian, C.D.Swift and J.R.Murray. UCRL-TR-234110LRD. 85, 342 **(2007)**
[6]   Y.Lin, T.J.Kessler, J.J.Armstrong. SPIE. 1870, **(1993)**
[7]   Y.Lin, T.J.Kessler, G.N.Lawrence. Appl. Opt. 21, 33 **(1994)**
[8]   Lv Baida, Transmission and control of high power laser, National Defense Industry Press, Beijing **(1999)**
[9]   Du Xiangwan. Chinese Journal of Lasers. 4, 24 **(1997)**
[10] Liu Zejin, Zhou Pu, Xu Xiaojun. Chinese Journal of Lasers. 4, 36 **(2009)**
[11] Luo Xi, Investigation on the Propagation and Transformation and Beam Control of High-Power Lasers, Ph.D thesis of Huazhong University of Seience & Technology, Wuhan **(2011)**
[12] Wei Xiaohong, Optical beam quality and transfer characteristics of high Power laser in nonlinear processes, Ph.D thesis of Fudan University, Shanghai **(2009)**
[13] M. G. Raymer, J. Mostowski, Physical Review A. 24 **(1981)**